applied sciences

Article

An Effect of MHD on Non-Newtonian Fluid Flow over a Porous Stretching/Shrinking Sheet with Heat Transfer

Angadi Basettappa Vishalakshi [1], Thippaiah Maranna [1], Ulavathi Shettar Mahabaleshwar [1] and David Laroze [2,*]

1 Department of Mathematics, Shivagangotri, Davangere University, Davangere 577007, India; vishalavishu691@gmail.com (A.B.V.); marannat4@gmail.com (T.M.); u.s.m@davangereuniversity.ac.in (U.S.M.)
2 Instituto de Alta Investigación, Universidad de Tarapacá, Casilla 7D, Arica 1000000, Chile
* Correspondence: dlarozen@uta.cl

Abstract: The current article explains the 3-D MHD fluid flow under the impact of a magnetic field with an inclined angle. The porous sheet is embedded in the flow of a fluid to yield the better results of the problem. The governing PDEs are mapped using various transformations to convert in the form of ODEs. The yielded ODEs momentum equation is examined analytically to derive the mass transpiration and then it is used in the energy equation and solved exactly by using various controlling parameters. In the case of multiple solutions, the closed-form exact solutions of highly non-linear differential equations of the flow are presented as viscoelastic fluid, which is classified as two classes, namely the second order liquid and Walters' liquid B fluid. The results can be obtained by using graphical arrangements. The current work is utilized in many real-life applications, such as automotive cooling systems, microelectronics, heat exchangers, and so on. At the end of the analysis, we concluded that velocity and mass transpiration was more for Chandrasekhar's number for both the stretching and shrinking case.

Keywords: Walters' liquid B; inclined MHD; similarity transformation; porous media; heat transfer; radiation

check for updates

Citation: Vishalakshi, A.B.; Maranna, T.; Mahabaleshwar, U.S.; Laroze, D. An Effect of MHD on Non-Newtonian Fluid Flow over a Porous Stretching/Shrinking Sheet with Heat Transfer. *Appl. Sci.* **2022**, *12*, 4937. https://doi.org/10.3390/app12104937

Academic Editors: Alexandre M. Afonso and Luís L. Ferrás

Received: 2 April 2022
Accepted: 10 May 2022
Published: 13 May 2022

1. Introduction

The challenges on stretching sheets are helpful for engineering and industrial applications for manufacturing plastic, polymers, and more. In the present paper we are discussing the three-dimensional flow over a porous body on the non-Newtonian fluid in the presence of MHD and an inclined angle. Sakiadis [1] examined the behavior of the laminar and turbulent boundary layer flow of continuously moving solid surface and flat surface. This work is extended by Crane [2], considering fluid with a stretching sheet, after experiencing many challenges conducted on stretching sheet problems. Andersson [3,4] has examined the problem with viscous flow with uniform magnetic field; this work is properly valid for any Reynolds number. Wang [5], studied the stagnation point flow. Fang and Zhang [6] examined the heat transfer analysis on the basis of an analytical method. Miklavcic and Wang [7] discussed the asymmetric cases of two-dimensional flow in the presence of a suction parameter with multiple solutions. Turkyilmazoglu et al. [8,9] worked on Jeffrey fluid with a stagnation point. Mahabaleshwar et al. [10] examined the problems on a stretching surface by considering MHD Newtonian hybrid nanofluid flow due to superlinear stretching sheet. Very recently, Vishalakshi et al. [11] studied the stretching sheet problem by using Rivlin-Ericksen fluid by using mass transpiration and thermal communication. Mahabaleshwar et al. [12] investigated stretching sheet problems by considering different aspects of parameters, such as the Brinkmann ratio, thermal radiation, porous medium parameter, and so on. Apart from these studies, some research was conducted on porous sheets while under the impact of magnetic parameter. Porous medium and magnetic parameters contributed a major role in the study of stretching sheet problems. There are many equations available to describe the porous medium. Many investigations conducted on porous medium occurred under the impact of a magnetic field. Khan et al. [13] worked on the fluid flow with MHD, as well as the transfer of mass with a porous medium. Nadeem et al. [14] worked on the numerical results of MHD Casson nanofluid. Mahabaleshwar [15] conducted the work on magneto-convection electrically conducting micropolar liquids. Mahabaleshwar et al. [16–18] worked on fluid flow with heat transfer by considering different fluids using different parameters in the presence of porous medium. Mahabaleshwar et al. [19–21] reviewed the flow of Casson fluid, couple stress fluid, and nanofluid with heat transfer under the impact of MHD with various parameters. See some the recent investigations on MHD and porous medium in [22–27].

Inspired by the above literatures, this current work is the study of 3-D flow with transpiration and radiation. The novelty of the present work is to explain the three-dimensional flow of a fluid with heat transfer under the impact of magnetic field and in the presence of a porous medium. Resulting ODEs are obtained by changing PDEs by using suitable variables. Analytical results can be conducted by using different controlling parameters. Temperature equations can be examined analytically and exhibit in gamma functions. Results can be obtained with the help of different physical parameters. The results of skin friction and Nusselt number is also discussed. The present work contains many industrial applications as well as its argument with the work of Vishalakshi et al. [28].

2. Problem Statement and Solution

A 3-D fluid flow was named Walter's liquid B, due to a porous sheet with inclined angle, transpiration, and thermal radiation. Fluid flow moved towards the x-axis and y-axis and was placed normally to it. Let σ indicate electrical conductivity, assuming the flow of a fluid, along with strength, B_0. A porous medium was placed inside the flow of a fluid and schematically the present flow was indicated in Figure 1.

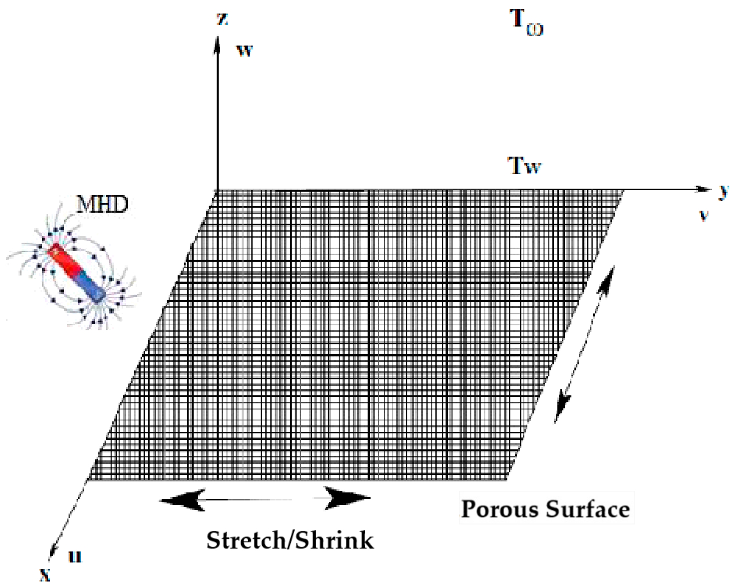

Figure 1. Schematic diagram of the three-dimensional flow.

Using these assumptions, the modelled governing equations are defined as follows [29–31]

$$u_x + v_y + w_z = 0, \tag{1}$$

$$\begin{aligned} uu_x + vu_y + wu_z = \quad & \nu u_{zz} - \left(\frac{\nu}{k_1} + \frac{\sigma {B_0}^2}{\rho}\sin^2(\tau)\right)u \\ & -k\{uu_{xzz} + wu_{zzz} - (u_x u_{zz} + u_z w_{zz} + 2u_z u_{xz} + 2w_z u_{zz})\} \end{aligned} \tag{2}$$

$$
\begin{aligned}
uv_x + vv_y + wv_z = \quad & \nu v_{zz} - \left(\frac{\nu}{k_1} + \frac{\sigma {B_0}^2}{\rho}\sin^2(\tau)\right)v \\
& -k\{vv_{xzz} + wv_{zzz} - (v_x v_{zz} + v_z w_{zz} + 2v_z v_{xz} + 2w_z v_{zz})\}
\end{aligned} \tag{3}
$$

$$
uT_x + vT_y + wT_z = \alpha T_{zz} - \frac{1}{\rho C_P}(q_r)_z, \tag{4}
$$

along with B. Cs (see [32])

$$
\left.
\begin{array}{c}
u = ax + lu_z,\ v = by + lv_z,\ w = w_0,\ at\ z = 0 \\
u \to 0,\ u_z \to 0,\ v \to 0, \quad as \quad z \to \infty
\end{array}
\right\} \tag{5}
$$

where, u, v, and w indicate the velocities along the x, y, and z direction, respectively, and τ indicates the inclined angle; ν is the kinematic viscosity, l indicates slip factor, ρ is the density, α is the thermal diffusivity, w_0 indicates wall transfer velocity, and k indicates permeability of the porous medium. Next we introduce the suitable variables as follows:

$$
\eta = \sqrt{\frac{|a|}{\nu}}z,\ u = |a|xf_\eta(\eta),\ v = |a|yg_\eta(\eta),\ w = -\sqrt{|a|\nu}(f(\eta) + g(\eta)) \tag{6}
$$

by using the similarity transformation Equation (1) converted as follows:

$$
\begin{aligned}
& f_{\eta\eta\eta} + (f+g)f_{\eta\eta} - {f_\eta}^2 - \left(Q\sin^2\tau + \frac{1}{Da}\right)f_\eta + \\
& K\left[(f+g)f_{\eta\eta\eta\eta} + (f_{\eta\eta} + g_{\eta\eta})f_{\eta\eta} - 2(f_\eta + g_\eta)f_{\eta\eta\eta}\right] = 0
\end{aligned} \tag{7}
$$

$$
\begin{aligned}
& g_{\eta\eta\eta} + (f+g)g_{\eta\eta} - {g_\eta}^2 - \left(Q\sin^2\tau + \frac{1}{Da}\right)g_\eta + \\
& K\left[(f+g)g_{\eta\eta\eta\eta} + (f_{\eta\eta} + g_{\eta\eta})g_{\eta\eta} - 2(f_\eta + g_\eta)g_{\eta\eta\eta}\right] = 0
\end{aligned} \tag{8}
$$

Therefore, B. Cs defined in Equation (5) becomes:

$$
f(0) = V_C,\ f_\eta(0) = d + \Gamma f_{\eta\eta}(0),\ g(0) = 0 \tag{9}
$$

$$
f_\eta(\infty) \to 0,\ f_{\eta\eta}(\infty) \to 0,\ g_\eta(\infty) \to 0,\ g_{\eta\eta}(\infty) \to 0 \tag{10}
$$

where the $d = \dfrac{b}{|a|}$ indicates stretching/shrinking sheet parameter, mass flux velocity is given by $V_C = -\dfrac{w_0}{\sqrt{|a|\nu}}$, viscoelasticity is $K = \dfrac{|a|k}{\nu}$, Chandrasekhar's number is to be $Q = \dfrac{\sigma B_0^2}{|a|\rho}$, Darcy number is $Da^{-1} = \dfrac{\nu}{k_1|a|}$, and $\Gamma = l\sqrt{\dfrac{|a|}{\nu}}$ is the velocity slip parameter.

3. Exact Solutions of Momentum Equation

Let us consider the solution of Equations (7) and (8) are as follows:

$$
f(\eta) = V_C + d\left(\frac{1 - \exp(-\lambda\eta)}{\lambda(1 + \Gamma\lambda)}\right),\ g(\eta) = d\left(\frac{1 - \exp(-\lambda\eta)}{\lambda(1 + \Gamma\lambda)}\right). \tag{11}
$$

where V_C indicates mass transpiration, if $V_C > 0$ indicates suction and $V_C < 0$ indicates injection.

By using the Equation (11) in Equations (7) and (8) to get the following resulting equations:

$$
\begin{aligned}
& 2K\lambda^2 - 1 = 0, \\
& (1 + \Gamma\lambda)\left(\left(Q\sin^2\tau + \frac{1}{Da}\right) - \lambda\left(V_C - \lambda + KV_C\lambda^2\right)\right) - 2d\left(1 + K\lambda^2\right) = 0,
\end{aligned} \tag{12}
$$

After solving Equation (7) we get:

$$\begin{aligned} &\lambda = \pm\frac{1}{\sqrt{2k_1}}, \\ &V_C = \frac{\left(Q\sin^2\tau + \frac{1}{Da}\right)(1+\Gamma\lambda) - 2d\left(1+K\lambda^2\right) + \lambda^2(1+\Gamma\lambda)}{\lambda(1+K\lambda^2)(1+\Gamma\lambda)}, \end{aligned} \tag{13}$$

Skin friction co-officiants are also modified in the following form:

$$f_{\eta\eta}(0) = g_{\eta\eta}(0) = -\frac{d\lambda}{1+\Gamma\lambda}. \tag{14}$$

4. Exact Solutions of Energy Equation

This problem is essentially forced into a convection problem with the following boundary conditions:

$$\begin{aligned} T &= T_w, \text{ at } z = 0 \\ T &\to T_\infty \text{ as } z \to \infty. \end{aligned} \tag{15}$$

By using Rosseland's approximation, q_r is defined as follows (see Mahabaleshwar et al. [33–35]):

$$q_r = \frac{-4\sigma^*}{3k^*}\left(\frac{\partial T^4}{\partial z}\right). \tag{16}$$

where σ^* is the Stefan-Boltzmann constant, k^* is the coefficient of mean absorption, and T is the temperature of the fluid.

The term T^4 can be expanded as

$$T^4 = T_\infty^4 + 4T_\infty^3(T - T_\infty) + 6T_\infty^2(T - T_\infty)^2 + \ldots\ldots, \tag{17}$$

some higher order series ignore to get the result as:

$$T^4 = -3T_\infty^4 - 4T_\infty^3 T. \tag{18}$$

Using Equation (18) in Equation (16) to yield the result as:

$$\frac{\partial q_r}{\partial y} = -\frac{16\sigma^* T_\infty^3}{3k^*}\frac{\partial^2 T}{\partial y^2}. \tag{19}$$

By using the transformations defined in Equations (6) and (19) in Equation (4) to yield the following result:

$$\omega\theta_{\eta\eta}(\eta) + Pr(f(\eta) + g(\eta))\theta_\eta(\eta) = 0, \tag{20}$$

where $f(\eta)$ is given in Equation (11), we consider $\omega = \frac{3N+4}{3N}$, $N = \frac{-4\sigma^* T_\infty^3}{3k^*\kappa_f}$, and $Pr = \frac{\kappa_f}{\mu C_p}$.

Then the corresponding boundary conditions become:

$$\theta(0) = 1,\ \theta(\infty) \to 0\}, \tag{21}$$

To derive a homogeneous equation of Equation (19) by the use of power series method. The solution is $\theta(t) = \sum_{t=0}^{\infty} a_r t^{m+r}$, where a_r is the arbitrary constant and m is the constants to be determined.

Where:

$$t = \frac{2dk_1 Pre^{-\lambda\eta}}{1+\Gamma\lambda} \tag{22}$$

On substituting t and also solving Equation (20) by using the B. Cs of Equation (21) to yield the following results:

$$\theta(\eta) = C_1 + C_2\Gamma\left(\frac{2}{3\omega}\left(1 - 2K\left(Q\sin^2(\tau) + Da^{-1}\right)\right), \frac{4dK\mathrm{Pr}e^{-\frac{\eta}{\sqrt{2}\sqrt{K}}}}{1 + \frac{\Gamma}{\sqrt{2}\sqrt{K}}}\right) \tag{23}$$

$$\theta(\eta) = \frac{\Gamma\left(\frac{2}{3\omega}\left(1 - 2K\left(Q\sin^2(\tau) + Da^{-1}\right)\right), 0\right) - \Gamma\left(\frac{2}{3\omega}\left(1 - 2K\left(Q\sin^2(\tau) + Da^{-1}\right)\right), \frac{4dK\mathrm{Pr}e^{-\frac{\eta}{\sqrt{2}\sqrt{K}}}}{1+\frac{\Gamma}{\sqrt{2}\sqrt{K}}}\right)}{\Gamma\left(\frac{2}{3\omega}\left(1 - 2K\left(Q\sin^2(\tau) + Da^{-1}\right)\right), 0\right) - \Gamma\left(\frac{2}{3\omega}\left(1 - 2K\left(Q\sin^2(\tau) + Da^{-1}\right)\right), \frac{4dK\mathrm{Pr}}{1+\frac{\Gamma}{\sqrt{2}\sqrt{K}}}\right)} \tag{24}$$

5. Results and Discussion

In the current study, we emphasize the investigation on fluid flow with heat transfer under the impact of an inclined angle, Chandrasekhar's number transpiration, and radiation. The PDEs of the problem are mapped into ODEs using suitable transformations, then the resulting ODEs are solved analytically. Multiple solutions are used to analyse the present study. The analytical results of the momentum and energy equation is obtained at Equations (13) and (24), and the results of the momentum equation are obtained in terms of mass transpiration. The solution domain λ linked with another parameters through Equation (13). Analytical results of momentum and energy equation is, respectively, represented at Equations (13) and (24). By using graphical arrangements, the impact of different parameters can be performed.

Figure 2a,b exhibits the impact of $f(\eta)$ on η for various choices of Q for $d = 1$ and $d = -1$, respectively, and keeping other parameters as $\tau = 90°$, $k_1 = 1$, and $Da = 0.3$. Here, blue solid lines indicate the $\Gamma = 1$, and black dotted lines indicate the $\Gamma = 0$. From this graph, it is cleared that $f(\eta)$ is for values of Q for both $d = 1$ and $d = -1$. Figures 3 and 4 portray the effect of $f_\eta(\eta)$ on η for different choices of Γ and k_1, respectively. Figure 3a,b indicate the plots of $f_\eta(\eta)$ verses η for different choices of Γ for $d = 1$ and $d = -1$, respectively, in this $f_\eta(\eta)$ less for more values of Γ for $d = 1$. It is opposite if $d = -1$, i.e., $f_\eta(\eta)$ is for more values of Γ for $d = -1$. Figure 4a,b indicate the plots of $f_\eta(\eta)$ verses η for various values of k_1 for $d = 1$ and $d = -1$, respectively, in this t is observed that $f_\eta(\eta)$ is more for more choices of k_1 for $d = 1$. This impact is opposite if $d = -1$. i.e., $f_\eta(\eta)$ less for more values of k_1 for $d = -1$. In this problem we express the analytical method in terms of mass transpiration and the domain linked with other parameters through this equation.

Figure 5a,b portrays the plots of V_C verses k_1 for different choices of Q for $d = 1$ and $d = -1$, respectively, and keeps the other parameters as $\tau = 90^{\circ}$, $Da = 0.3$. Here, blue solid lines indicate the $\Gamma = 2$ and black dotted lines indicate the $\Gamma = 0$. λ value connected with k_1 through Equation (13). In these graphs V_C is for values of Q for both $d = 1$ and $d = -1$.

Figure 6a,b demonstrated the impact of $\theta(\eta)$ on η for different values of Q for $d = 1$ and $d = -1$. In this $\theta(\eta)$ is for values of Q for both $d = 1$ and $d = -1$. Figure 7a,b demonstrated the impact of $\theta(\eta)$ on η for various choices of N for $d = 1$ and $d = -1$, in this it is observed that $\theta(\eta)$ is decreased for increasing the N for both $d = 1$ and $d = -1$. In these graphs it is observed that there is little difference between $d = 1$ and $d = -1$. In these figures, it is carefully observed that boundary value thickness is wider for the shrinking sheet case when compared to the stretching sheet case. Boundary value thickness is the velocity boundary layer; it is normally as the distance from the solid body.

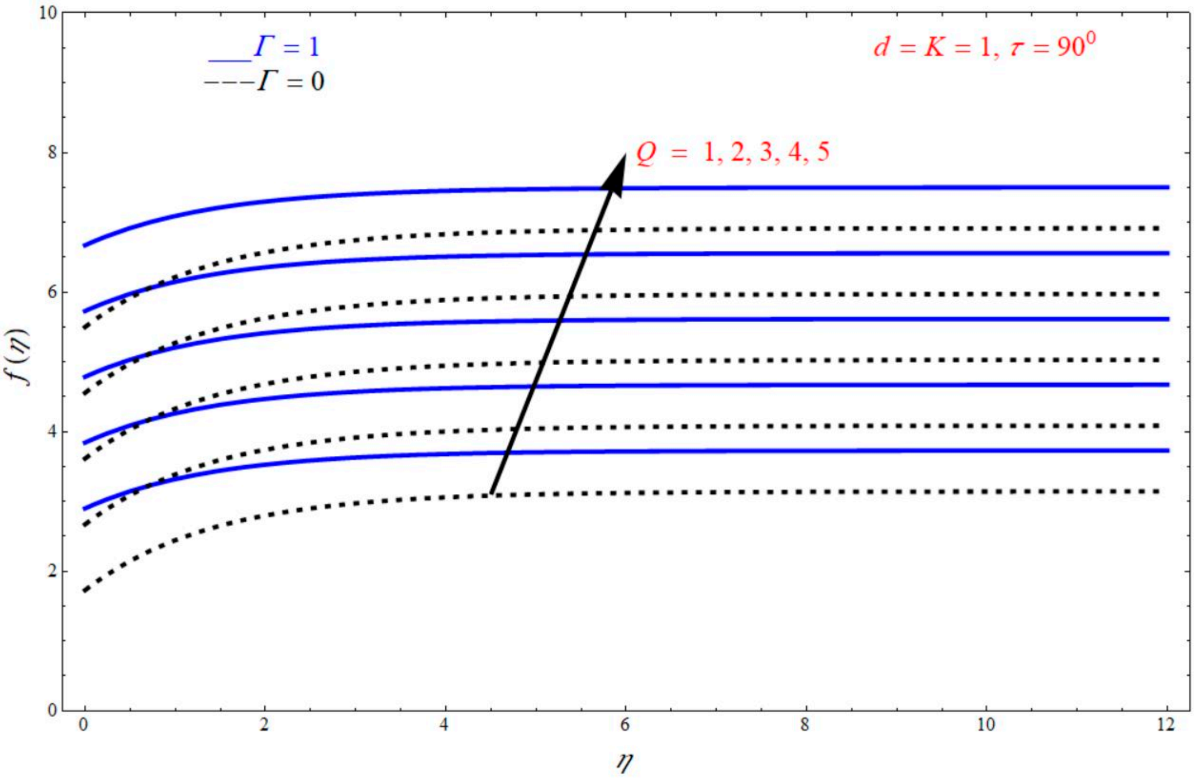

(**a**)

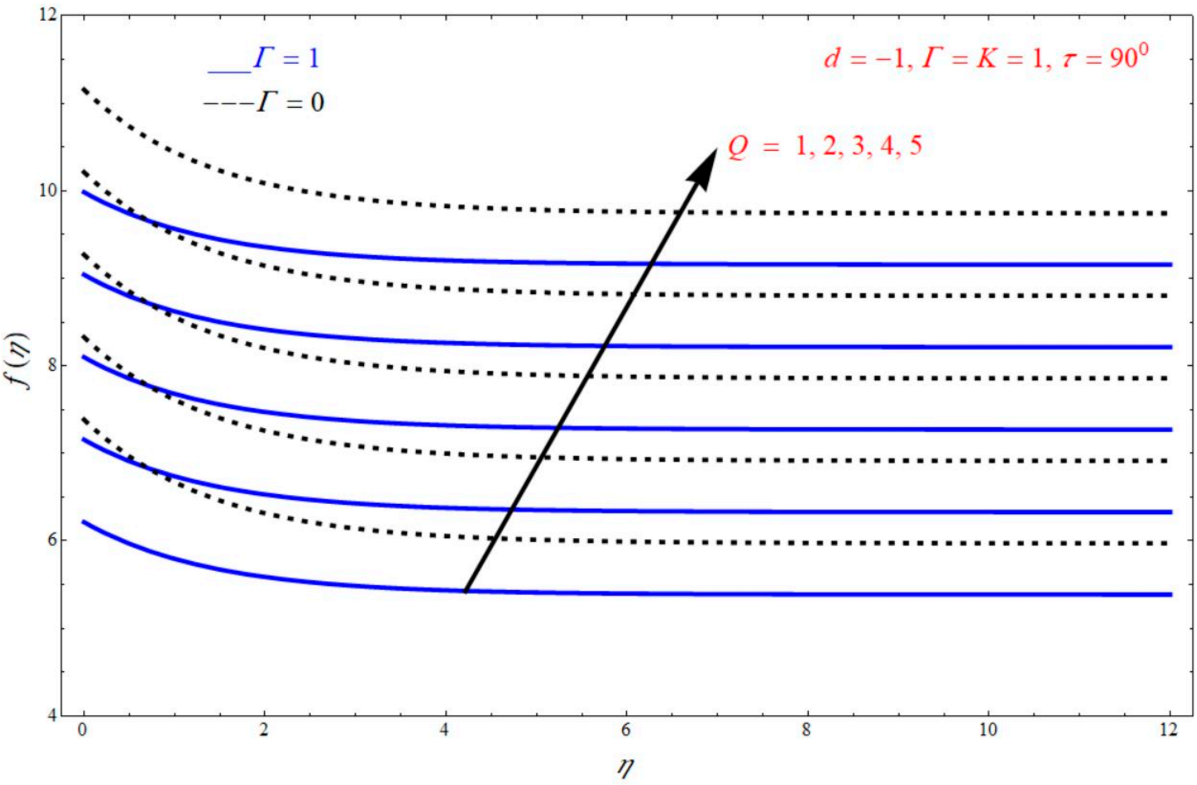

(**b**)

Figure 2. Impact of $f(\eta)$ on η for various choices of Q for (**a**) $d = 1$ and (**b**) $d = -1$.

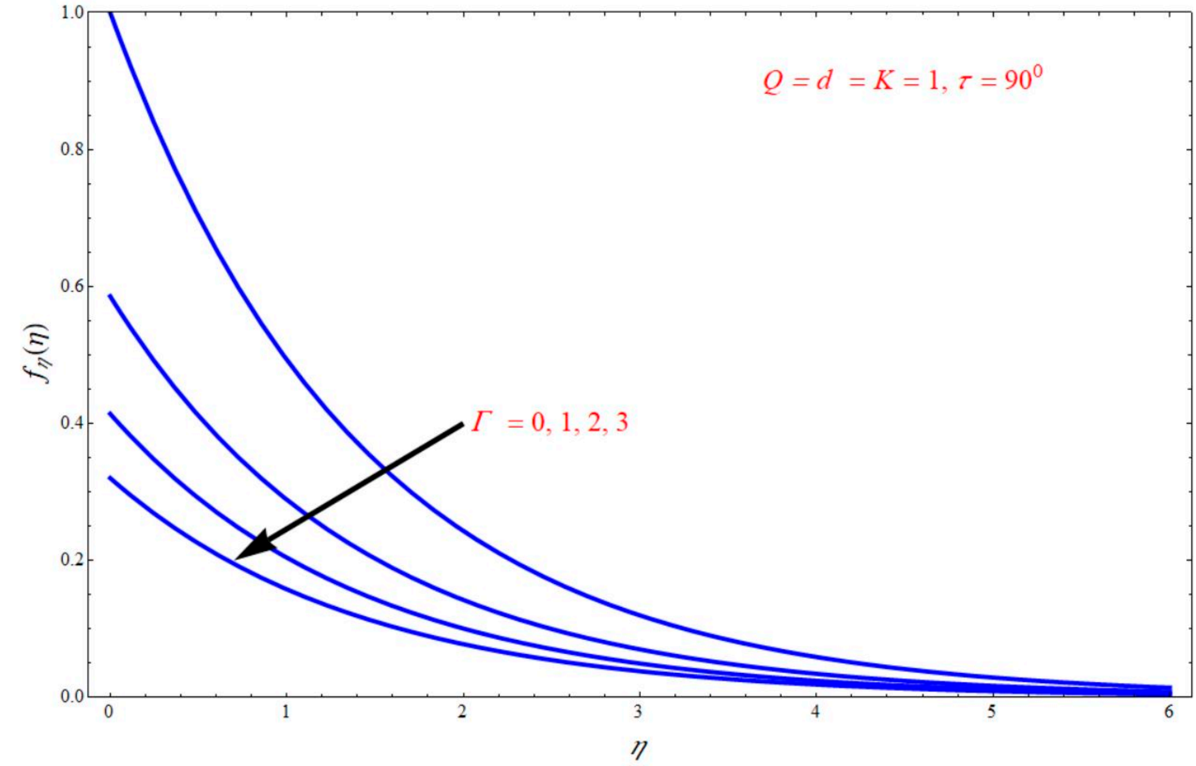

(**a**)

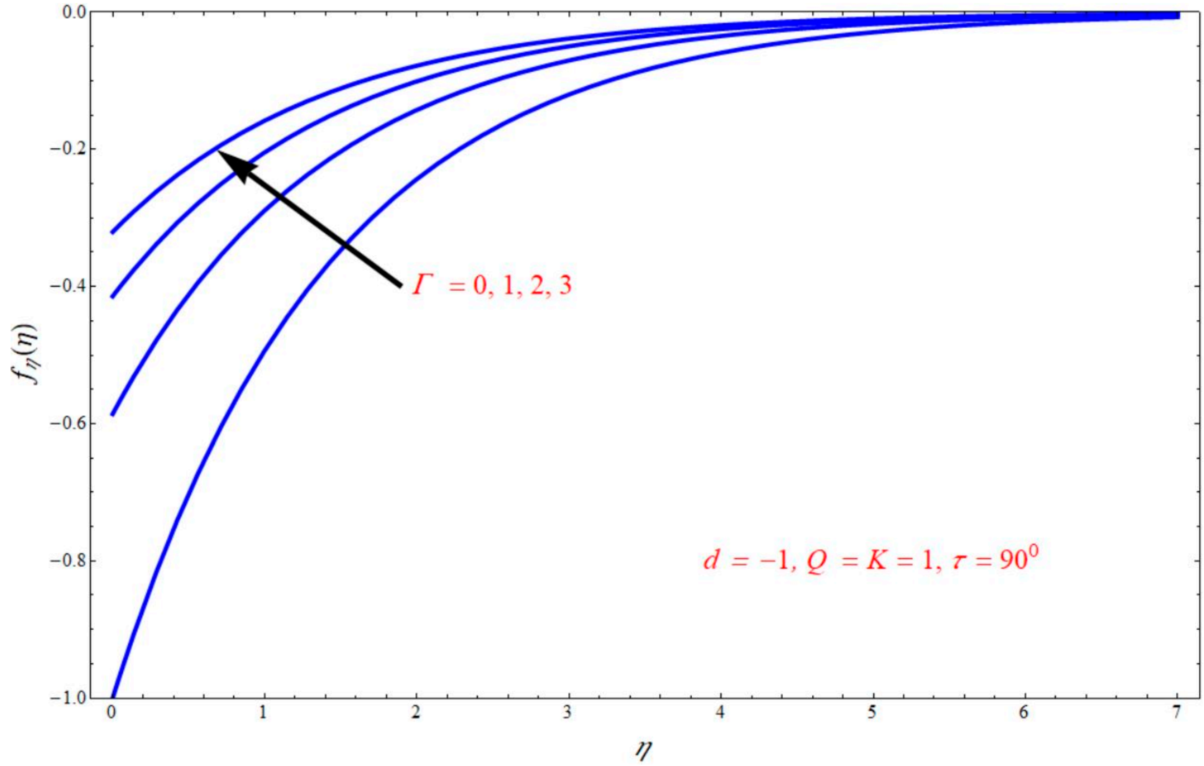

(**b**)

Figure 3. Plots of $f_\eta(\eta)$ verses η for different values of Γ for both (**a**) $d = 1$ and (**b**) $d = -1$.

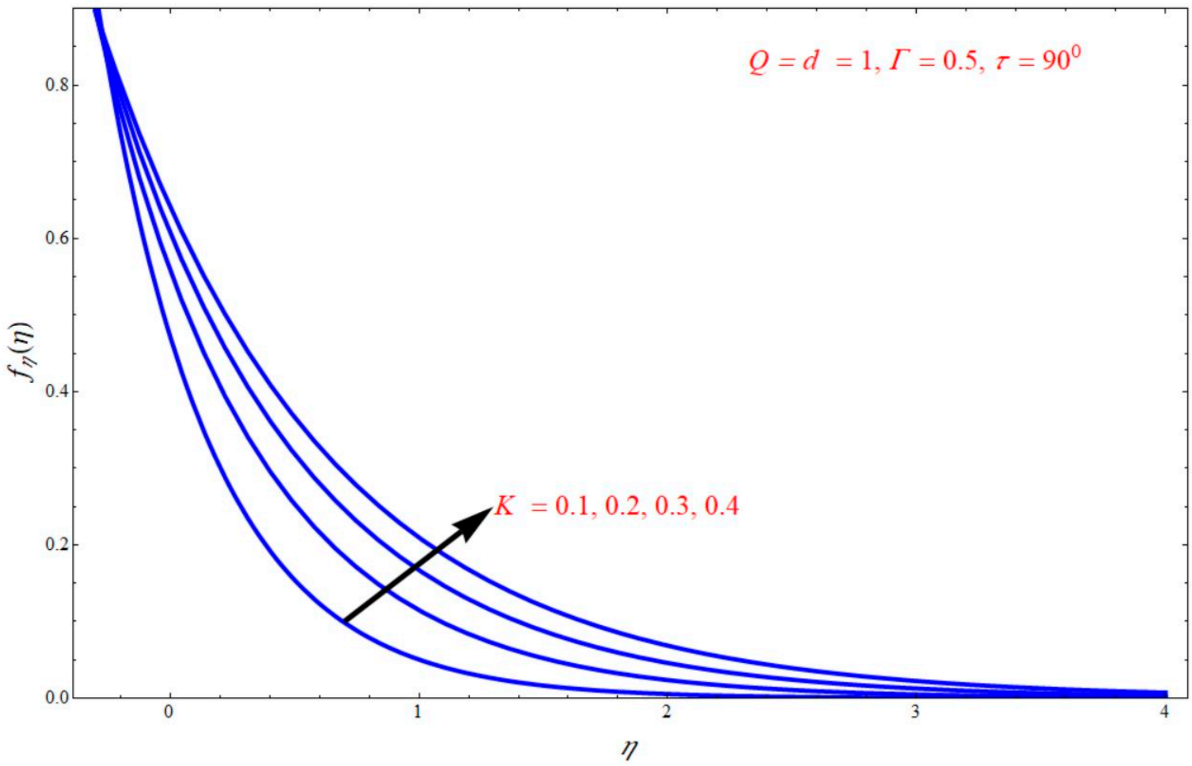

(**a**)

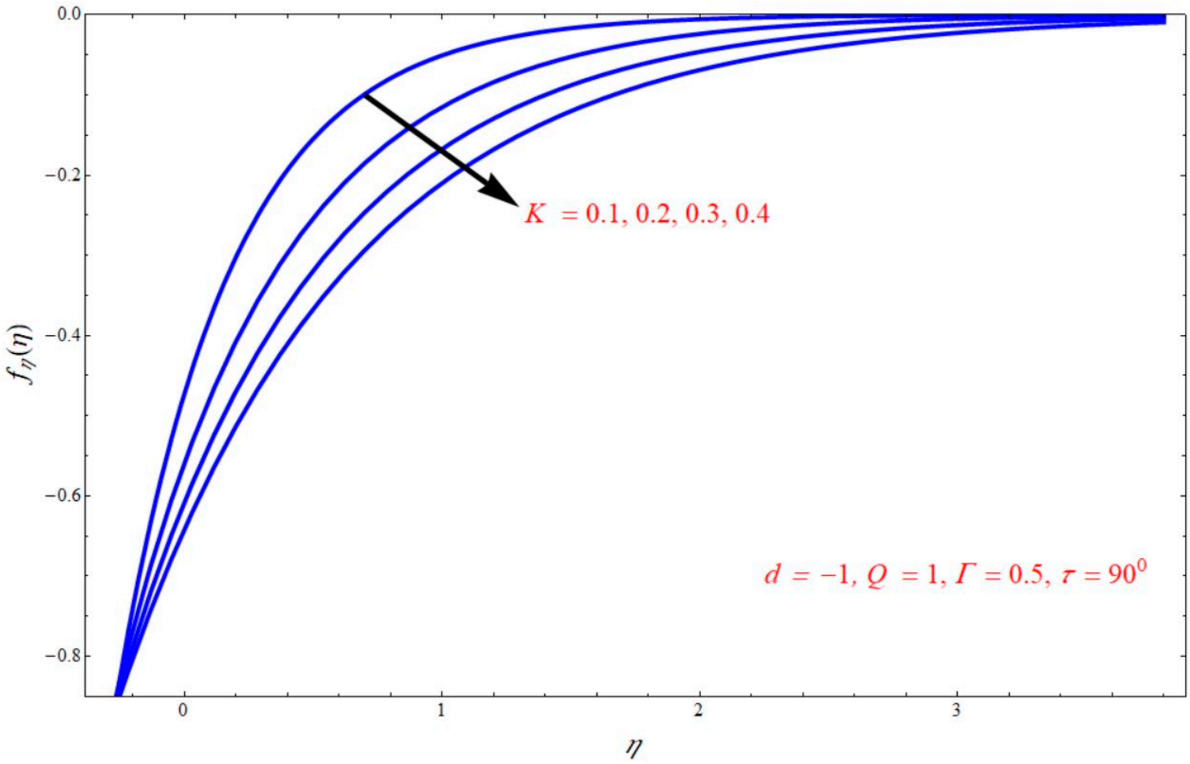

(**b**)

Figure 4. Plots of $f_\eta(\eta)$ verses η for different choices of k_1 for (**a**) $d = 1$ and (**b**) $d = -1$.

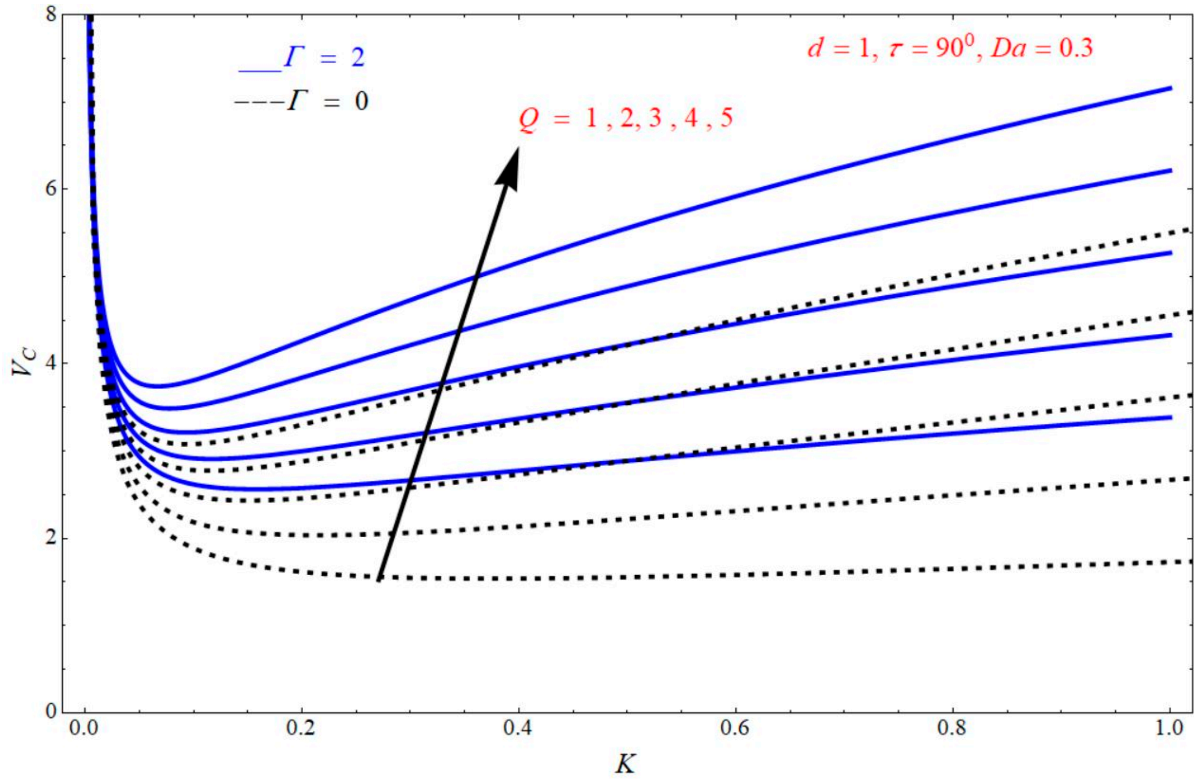

(**a**)

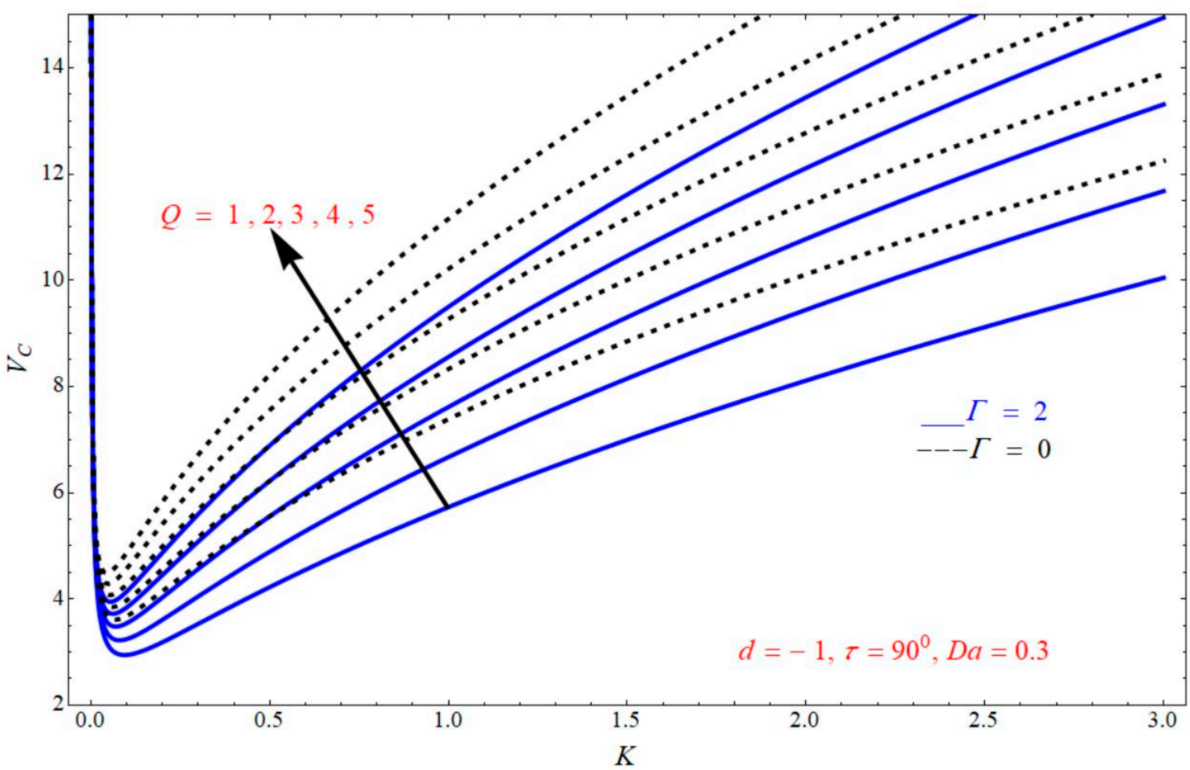

(**b**)

Figure 5. Impact of V_C on K for different values of Q for both (**a**) $d = 1$ and (**b**) $d = 1$.

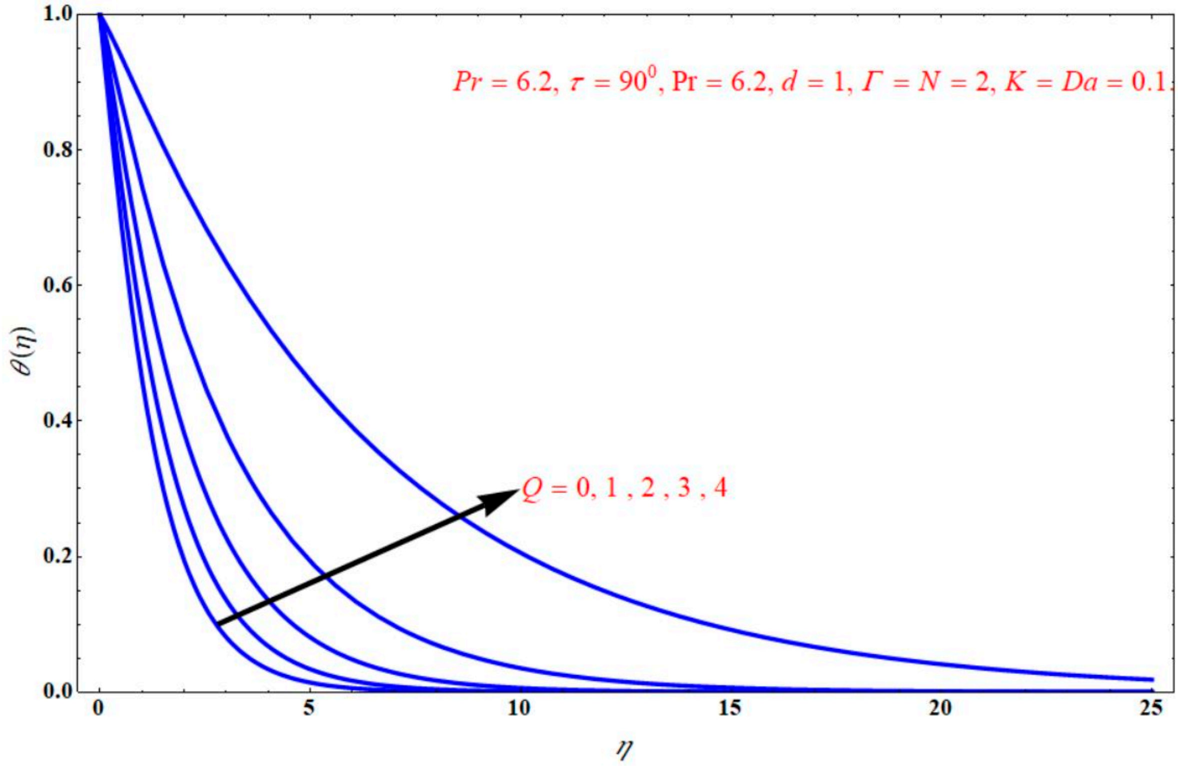

(**a**)

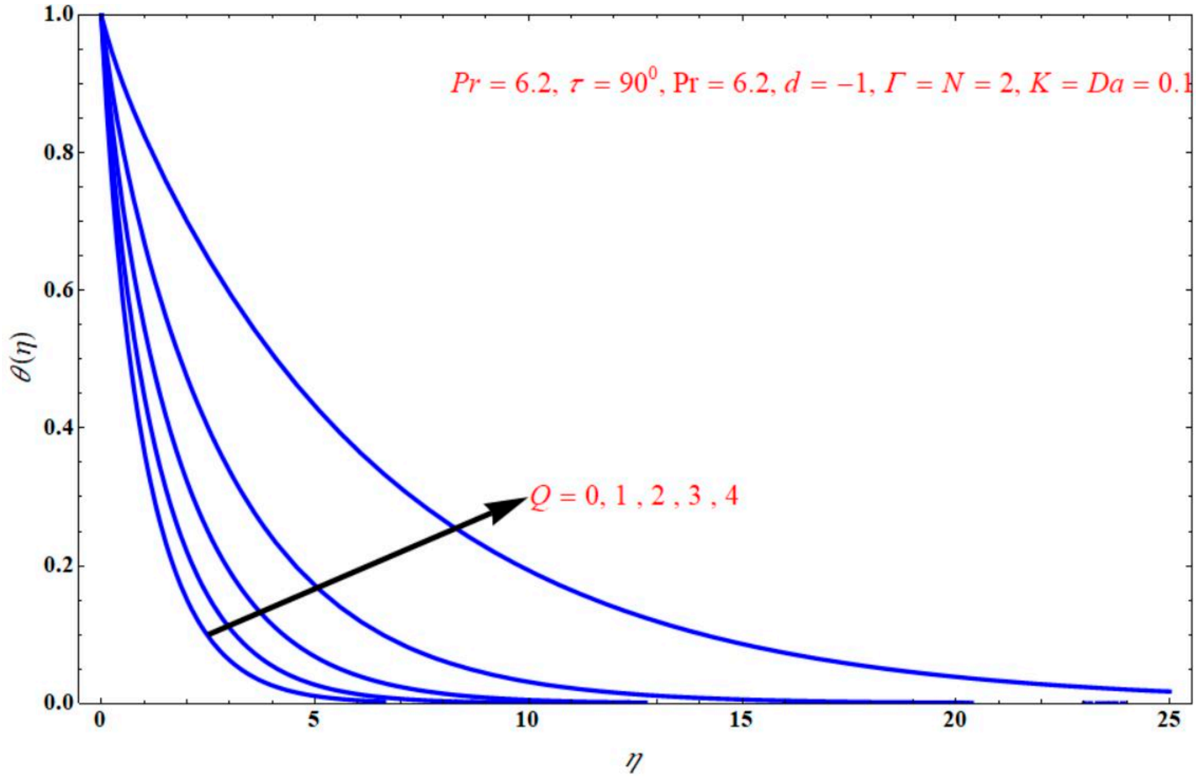

(**b**)

Figure 6. The plots of $\theta(\eta)$ verses η for different choices of Q for (**a**) $d = 1$ and (**b**) $d = -1$.

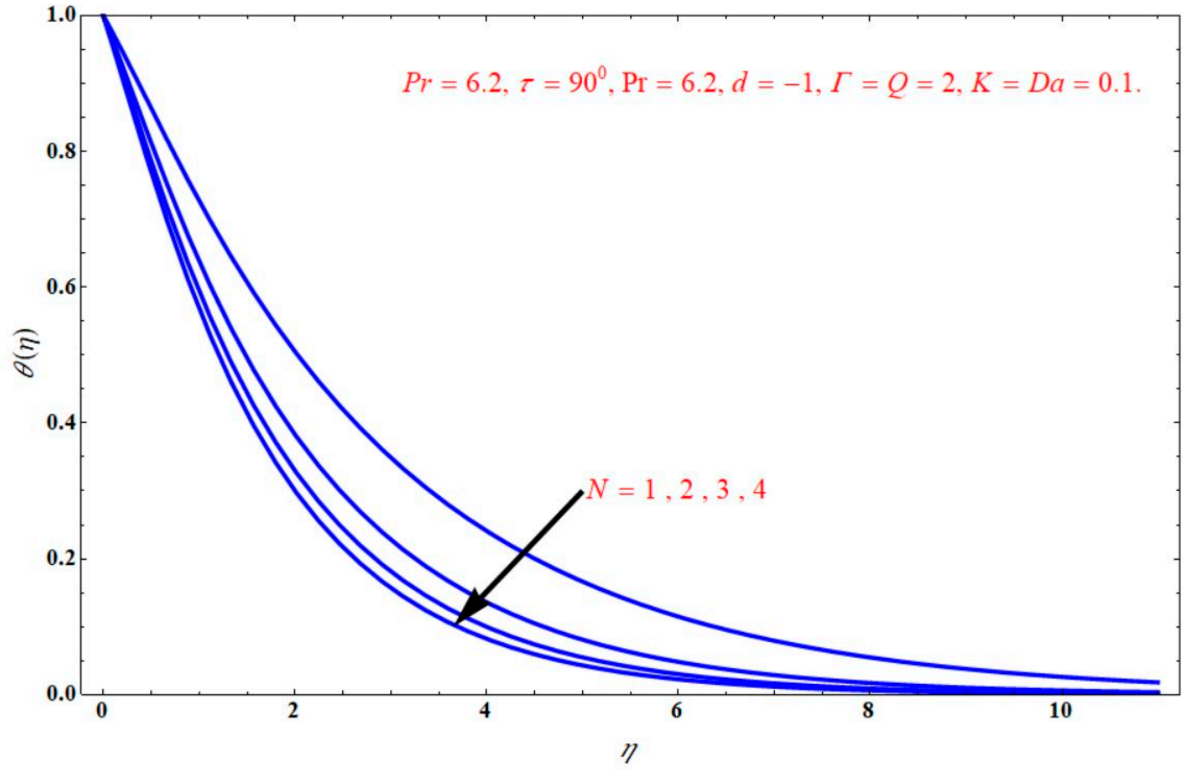

(**a**)

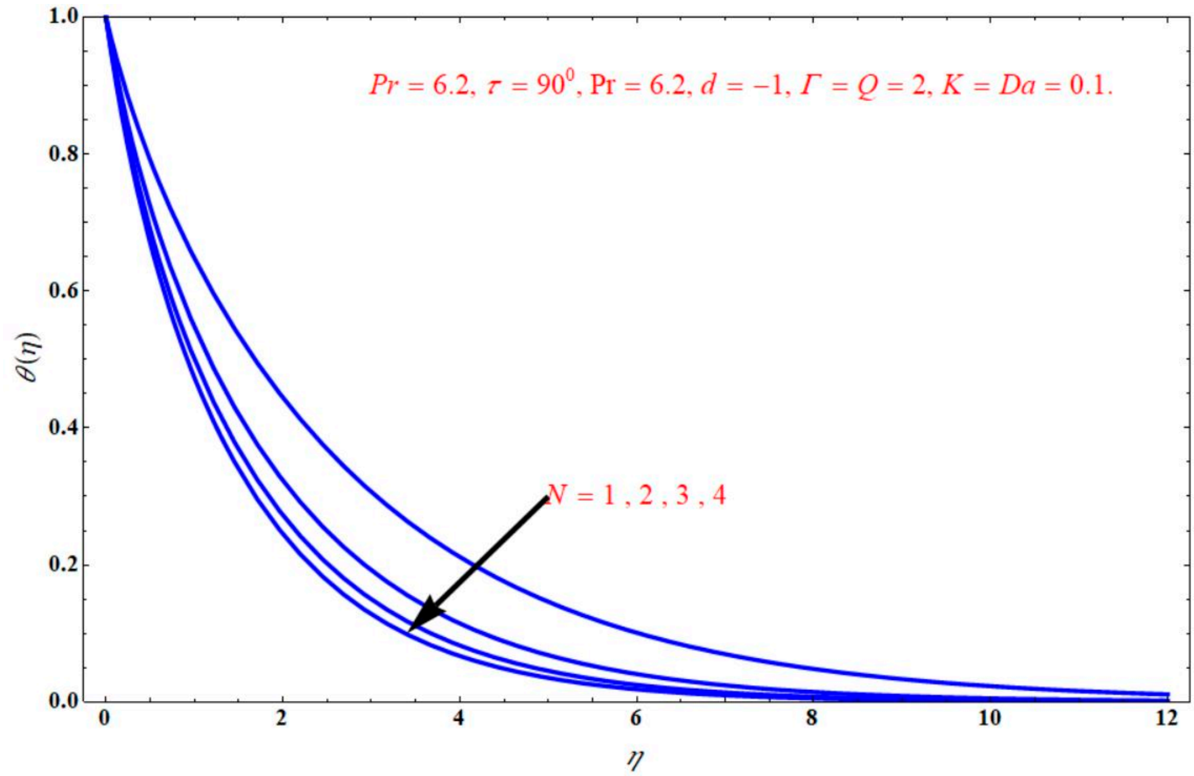

(**b**)

Figure 7. Impact of $\theta(\eta)$ on η for various choices of Q for both (**a**) $d = 1$ and (**b**) $d = -1$.

6. Concluding Remarks

A steady 3-D fluid flow over a porous sheet was taken to analyse the present study under the impact of inclined magnetic field. Multiple slips are considered in the current study to yield better results to the problem. The PDEs of the current problem were mapped into ODEs using suitable variables. Then, analytical solutions were obtained using various parameters. Graphical representations were achievable by using different parameters. With the graphical arrangements, the following results can be deduced:

$f(\eta)$ is for values of Q for both $d = 1$, and $d = -1$.

$f_\eta(\eta)$ less for values of Γ for $d = 1$. Also, it is for values of Γ for $d = -1$.

$f_\eta(\eta)$ increases with increased choices of k_1 for $d = 1$, but it decreases with increasing the values of k_1 for shrinking sheet condition.

V_C is for values of Q for both $d = 1$ and $d = -1$.

If $\tau = 0,\ \phi = 0,\ Bi \to \infty$ to get the results of Vishalakshi et al. [28].

If $Q = \beta = Da^{-1} = R = L = \tau = 0.$ to get the results of classical Crane [2].

Author Contributions: Conceptualization: U.S.M.; methodology: U.S.M. and D.L.; software: A.B.V. and T.M.; formal analysis: A.B.V., T.M. and U.S.M.; investigation: A.B.V., T.M., U.S.M. and D.L.; writing—original draft preparation: U.S.M.; writing—review and editing: D.L. All authors have read and agreed to the published version of the manuscript.

Funding: D.L. acknowledges partial financial support from Centers of Excellence with BASAL/ANID financing, Grant Nos. AFB180001, CEDENNA.

Institutional Review Board Statement: Not available.

Informed Consent Statement: Not available.

Data Availability Statement: Data sharing is not applicable to this article.

Conflicts of Interest: The authors have no conflict to disclose.

Nomenclature

a and b	Stretching/shrinking sheet coefficient constant $\left[s^{-1}\right]$
B_0	Strength of the magnetic field $\left[wm^{-2}\right]$
C_P	Specific heat $\left[JKg^{-1}K^{-1}\right]$
d	Length scale $[-]$
Da	Darcy number $[-]$
Q	Chandrasekhar's number $[-]$
Pr	Prandtl number $[-]$
k_1	Permeability of porous medium m^2
k	Material constant of fluid $[-]$
K	Viscoelasticity $[-]$
l	Slip factor $[-]$
m	Constants to be determined $[-]$
N	Radiation parameter $[-]$.
q_r	Heat flux $\left[Wm^{-2}\right]$
T	Fluid temperature $[K]$
T_w	Wall temperature $[K]$
T_∞	For field temperature $[K]$
u v and w	Axial velocity towards x axis $\left[ms^{-1}\right]$
V_C	Mass transpiration $[-]$
w_0	Wall transfer velocity $[mg]$
x, y and z	Coordinates $[m]$

Greek symbols

α	Thermal diffusivity $\left[m^2 s^{-1}\right]$
η	Similarity variable $[-]$
Γ	Parameter of the analytical solution $[-]$
λ	Constant domain $[-]$
ν	Kinematic viscosity $\left[m^2 s^{-1}\right]$
ρ	Density $\left[kgm^{-3}\right]$
σ	Electrical conductivity $\left[S\,m^{-1}\right]$
τ	Inclined angle [Rad]
θ	Scaled fluid temperature [K]
∞	Away from the sheet $[-]$
γ_0	Porosity $[p \cdot u]$
Abbreviations	
BCs	Boundary conditions $[-]$
MHD	Magnetohydrodynamics
ODEs	Ordinary differential equations $[-]$
PDEs	Partial differential equations $[-]$

References

1. Sakiadis, B.C. Boundary layer behaviour on continuous solid surfaces: I boundary layer equations for two dimensional and axisymmetric flow. *AIChE J.* **1961**, *7*, 26–28. [CrossRef]
2. Crane, L.J. Flow past a stretching plate. *Z. Angew. Math. Phys.* **1970**, *21*, 645–647. [CrossRef]
3. Andersson, H.I. An exact solution of the Navier-Stokes equations for magnetohydrodynamics flow. *Acta Mech.* **1995**, *113*, 241–244. [CrossRef]
4. Andresson, H.I. Slip flow past a stretching surface. *Acta Mech.* **2002**, *158*, 121–125. [CrossRef]
5. Wang, C.Y. Stagnation flow towards a shrinking sheet. *Int. J. Non-Linear Mech.* **2008**, *43*, 377–382. [CrossRef]
6. Fang, T.G.; Zhang, J. Thermal boundary layers over a shrinking sheet: An analytical solution. *Acta Mech.* **2010**, *209*, 325–343. [CrossRef]
7. Miklavcic, M.; Wang, C.Y. Viscous flow due to a shrinking sheet. *Q. Appl. Math.* **2006**, *64*, 283–290. [CrossRef]
8. Turkyilmazoglu, M. Multiple solutions of heat and mass transfer of MHD slip flow for the viscoelastic fluid over a stretching sheet. *Int. J. Therm. Sci.* **2011**, *50*, 2264–2276. [CrossRef]
9. Turkyilmazoglu, M.; Pop, I. Exact analytical solutions for the flow and heat transfer near the stagnation point on a stretching/shrinking sheet in a Jeffrey fluid. *Int. J. Heat Mass Transfer.* **2013**, *57*, 82–88. [CrossRef]
10. Mahabaleshwar, U.S.; Anusha, T.; Hatami, M. The MHD Newtonian hybrid nanofluid flow and mass transfer analysis due to super-linear stretching sheet embedded in porous medium. *Sci. Rep.* **2021**, *11*, 22518. [CrossRef]
11. Vishalakshi, A.B.; Mahabaleshwar, U.S.; Sheikhnejad, Y. Impact of MHD and mass transpiration on Rivlin-Ericksen liquid flow over a stretching sheet in a porous media with thermal communication. *Transp. Porous Media* **2022**, *142*, 353–381. [CrossRef]
12. Mahabaleshwar, U.S.; Vishalakshi, A.B.; Azese, M.N. The role of Brinkmann ratio on non-Newtonian fluid flow due to a porous shrinking/stretching sheet with heat transfer. *Eur. J. Mech. B/Fluids* **2022**, *92*, 153–165. [CrossRef]
13. Nadeem, S.; Haq, R.U.I.; Akbar, N.S.; Khan, Z.H. MHD three dimensional Casson fluid flow past a porous linearly stretching sheet. *Alex. Eng. J.* **2013**, *52*, 577–582. [CrossRef]
14. Mahabaleshwar, U.S.; Pažanin, I.; Radulović, M.; Suarez-Grau, F.J. Effects of small boundary perturbation on the MHD duct flow. *Theor. Appl. Mech.* **2017**, *44*, 83–101.
15. Mahabaleshwar, U.S. Combined effect of temperature and gravity modulations on the onset of magneto-convection in weak electrically conducting micropolar liquids. *J. Eng. Sci.* **2007**, *45*, 525–540. [CrossRef]
16. Mahabaleshwar, U.S.; Sarris, I.E.; Lorenzini, G. Effect of radiation and Navier slip boundary of Walters' liquid B flow over stretching sheet in a porous media. *Int. J. Heat Mass Transf.* **2018**, *17*, 1327–1337. [CrossRef]
17. Mahabaleshwar, U.S.; Nagaraju, K.R.; Sheremet, M.A.; Baleanu, D.; Lorenzini, E. Mass transpiration on Newtonian flow over a porous stretching/shrinking sheet with slip. *Chin. J. Phys.* **2020**, *63*, 130–137. [CrossRef]
18. Mahabaleshwar, U.S.; Nagaraju, K.R.; Kumar, P.N.V.; Nadagouda, M.N.; Bennacer, R.; Sheremet, M.A. Effect of Dufour and Soret mechanisms on MHD mixed convective—Radiative non-Newtonian liquid flow and heat transfer over a porous sheet. *Therm. Sci. Eng. Prog.* **2020**, *16*, 100459. [CrossRef]
19. Mahabaleshwar, U.S.; Rekha, M.B.; Vinay Kumar, P.N.; Selimefendigil, F.; Sakanaka, P.H.; Lorenzini, G.; Ravichandra Nayakar, S.N. Mass transfer characteristics of MHD Casson fluid flow past stretching/shrinking sheet. *J. Eng. Thermophys.* **2020**, *29*, 285–302. [CrossRef]
20. Mahabaleshwar, U.S.; Sarris, I.E.; Hill, A.A.; Lorenzini, G.; Pop, I. An MHD couple stress fluid due to a perforated sheet undergoing linear stretching with heat transfer. *Int. J. Heat Mass Transf.* **2017**, *105*, 157–167. [CrossRef]

21. Mahabaleshwar, U.S.; Kumar, P.N.V.; Sheremet, M. *Magnetohydrodynamics Flow of a Nanofluid Driven by a Stretching/Shrinking Sheet with Suction*; Springer: Berlin/Heidelberg, Germany, 2016; p. 1901.
22. Sneha, K.N.; Mahabaleshwar, U.S.; Chan, A.; Hatami, M. Investigation of radiation and MHD on non-Newtonian fluid flow over a stretching/shrinking sheet with CNTs and mass transpiration. *Waves Random Complex Media* **2022**, 1–20. [CrossRef]
23. Anusha, T.; Mahabaleshwar, U.S.; Hatami, M. Navier slip effect on the thermal flow of Walter's liquid B flow due to porous stretching/shrinking with heat and mass transfer. *Case Stud. Therm. Eng.* **2021**, *28*, 101691. [CrossRef]
24. Anusha, T.; Mahabaleshwar, U.S.; Sheikhnejad, Y. An MHD of nanofluid flow over a porous stretching/shrinking plate with mass transpiration and Brinkman ratio. *Transp. Porous Media* **2021**, *142*, 333–352. [CrossRef]
25. Anusha, T.; Huang, H.; Mahabaleshwar, U.S. Two dimensional unsteady stagnation point flow of Casson hybrid nanofluid over a permeable flat surface and heat transfer analysis with radiation. *J. Taiwan Inst. Chem. Eng.* **2021**, *127*, 79–91. [CrossRef]
26. Kumar, P.N.V.; Mahabaleshwar, U.S.; Swaminathan, N.; Lorenzini, G. Effect of MHD and mass transpiration on a viscous liquid flow past porous stretching sheet with heat transfer. *J. Eng. Thermophys.* **2021**, *30*, 404–419. [CrossRef]
27. Li, Z.; Barnoon, P.; Davood, T.; Dehkordi, R.B.; Afrand, M. Mixed convection of non-Newtonian nanofluid in an H-Shaped cavity with coolar and heater cylinders filled by a porous material: Two phase approach. *Fac. Eng. Inf. Sci. Pap. Part B* **2019**, *30*, 2666–2685.
28. Vishalakshi, A.B.; Mahabaleshwar, U.S.; Sarris, I.E. An MHD fluid flow over a porous stretching/shrinking sheet with slips and mass transpiration. *Micromachines* **2022**, *13*, 116. [CrossRef]
29. Rostami, S.; Davood, T.; Shabani, B.; Sina, N.; Barnoon, P. Measurement of the thermal conductivity of MWCNCT-CuO/Water hybrid nanofluid using artificial neural networks (ANNs). *J. Therm. Anal. Calorim.* **2021**, *143*, 1097–1105. [CrossRef]
30. Makarim, D.A.; Suami, A.; Wijayanta, A.T.; Kobayashi, N.; Itaya, Y. Marangoni convection within thermosolutal and absorptive aqueous LiBr solution. *Int. J. Heat Mass Transf.* **2022**, *188*, 122621.
31. Wijayanta, A.T. Numerical solution strategy for natural convection problems in a triangular cavity using a direct meshless local petrov-Galerkin method combined with an implicit artificial-compressibility model. *Eng. Anal. Bound. Elem.* **2021**, *126*, 13–29.
32. Rahmati, A.R.; Akbari, O.A.; Marzban, A.; Davood, T.; Farzad, R.K.P. Simultaneous investigations effects of non-Newtonian nanofluid flow in different volume fractions of solid nanoparticles with slip and no-slip boundary conditions. *Therm. Sci. Eng. Prog.* **2018**, *5*, 263–277. [CrossRef]
33. Mahabaleshwar, U.S.; Sneha, K.N.; Huang, H.N. An effect of MHD and radiation on CNTS-water based nanofluid due to a stretching sheet in a Newtonian fluid. *Case Stud. Therm. Eng.* **2021**, *28*, 101462. [CrossRef]
34. Mahabaleshwar, U.S.; Vishalakshi, A.B.; Andersson, H.I. Hybrid nanofluid flow past a stretching/shrinking sheet with thermal radiation and mass transpiration. *Chin. J. Phys.* **2022**, *75*, 152–168. [CrossRef]
35. Mahabaleshwar, U.S.; Anusha, T.; Sakanaka, P.H.; Bhattacharyya, S. Impact of Lorentz force and Schmidt number on chemically reactive Newtonian fluid flow on a stretchable surface when Stefan blowing and thermal radiation and significant. *Arab. J. Sci. Eng.* **2021**, *46*, 12427–12443. [CrossRef]